Theor Chem Acc (2011) 130:807–813
DOI 10.1007/s00214-011-1042-5

REGULAR ARTICLE

Theoretical investigation of hole mobility in 9,10-diphenylanthracene by density functional calculations

Shotaro Watanabe · Yasuyo Shimodo · Kenji Morihashi

Received: 12 June 2011 / Accepted: 12 September 2011 / Published online: 8 October 2011

Abstract The charge transfer property of the 9,10-diphenylanthracene (DPA) single-crystal system was investigated by density functional calculations. The hole mobility of DPA was predicted according to a hopping mechanism and compared with that of two standard organic single-crystal systems, namely, naphthalene and anthracene. The reorganization energy was calculated by the adiabatic potential energy surface method. The electronic coupling matrix elements were calculated by two methods, namely, the energy splitting in dimer (ESD) method and charge transfer integral (CTI) method. Using the coupling matrix calculated by the CTI method, we predicted a hole mobility of 2.15 $cm^2/(Vs)$ for DPA, whereas the CTI method gives the values of 0.35 and 1.39 $cm^2/(Vs)$ for naphthalene and anthracene, respectively. It is shown that the electronic coupling calculated by the CTI method gives the qualitatively satisfactory result for the hole mobilities of the three single-crystal systems.

Keywords Hole mobility · 9,10-Diphenylanthracene · Energy splitting in dimer · Charge transfer integral · DFT

Dedicated to Professor Akira Imamura on the occasion of his 77th birthday and published as part of the Imamura Festschrift Issue.

S. Watanabe · K. Morihashi (✉)
Department of Chemistry, Graduate School of Pure and Applied Sciences, University of Tsukuba, 1-1-1 Tennodai, Tsukuba, Ibaraki 305-8577, Japan
e-mail: morihasi@chem.tsukuba.ac.jp

Y. Shimodo
Faculty of Pharmacy, Yasuda Women's University, 6-13-1 Yasuhigashi, Asaminami-ku, Hiroshima 731-0153, Japan

1 Introduction

Organic semiconductors have attracted much attention owing to their possible application in electronic devices such as light-emitting diodes, field-effect transistors, and solar cells. The electric conductivity of organic materials is very important when electronic materials such as monocrystalline silicon and polycrystalline silicon are replaced with organic materials. Charge carrier mobility is an indicator that measures/determines conductivity of electronic materials. Numerous studies have been carried out to find/develop materials with high-charge carrier mobility [1, 2]. Therefore, a reliable method of predicting the mobility of various organic materials can serve as a useful screening tool for material and electronic device development. The incoherent hopping model proposed by Goddard and coworkers [3, 4] is considered to be one of the useful tools for predicting hole and electron mobilities [5, 6].

Recently, 9,10-diphenylanthracene (DPA) has attracted attention as an organic semiconductor with high electron and hole mobilities [7]. DPA has a substantially low vapor pressure at room temperature and a high-melting point and is thermally stable beyond the operating temperatures of thin-film transistors. In this paper, we focus on the hole-transfer property of DPA, and theoretically examine the origin of the good transport property of DPA using the hopping model. To clarify the transport property of DPA, we also used other organic single-crystal systems, i.e., naphthalene and anthracene. The structures of three molecules are shown in Fig. 1. As shown in Fig. 1, DPA has an interesting structure in which two phenyl groups are almost orthogonal to the anthracene backbone. A similar orthogonal π–system can also be seen in the structure of rubrene, whose crystal is a high-charge transfer material [8]. The hole-transfer properties of naphthalene, anthracene, and

DPA were investigated on the basis of the parameters obtained by density functional calculation. By a comparison among these three systems in Fig. 1, we examined how two phenyl groups introduced into DPA result in a good transport property.

2 Methods

In the incoherent transport model developed by Deng and Goddard [3], the charge diffusion coefficient D can be evaluated from the charge hopping rates as

$$D = \frac{1}{2n}\sum_i r_i^2 W_i P_i, \tag{1}$$

where n is the spatial dimension, which is equal to 3 for an organic crystal, i represents a specific hopping pathway (e.g., in the anthracene crystal case, hole transport occurs from the radical cation at the crystal center to the surrounding neutral molecules along eight hopping paths, T_1, T_2, P, and L, shown in Fig. 4), and r_i is defined as the mass center distance between the center and ith surrounding molecules. At room temperature, the charge hopping rate between neighboring molecules, W_i, is given by the Marcus–Hush equation [9, 10]

$$W_i = \frac{V_i^2}{\hbar}\left(\frac{\pi}{\lambda k_B T}\right)^{1/2} \exp\left(-\frac{\lambda}{4k_B T}\right), \tag{2}$$

where V_i is the electronic coupling between neighboring molecules in the organic single crystal, λ is the reorganization energy, k_B is the Boltzmann constant, and T is the temperature; $T = 300$ K was employed in the present calculations. Then, the relative probability for the ith pathway P_i is obtained as

$$P_i = W_i / \sum_i W_i. \tag{3}$$

In the hopping mechanism, the hole mobility μ is evaluated using the Einstein relation

$$\mu = \frac{e}{k_B T} D. \tag{4}$$

Quantum mechanical (QM) calculations are used to estimate reorganization energy and electronic coupling.

2.1 Reorganization energy

The reorganization energy for charge transfer (CT) consists of the internal and external contributions, i.e., $\lambda = \lambda_i + \lambda_e$ [11]. Neglecting the external contribution (effect of intermolecular interaction), $\lambda \sim \lambda_i$, the reorganization energy for a hole-transfer (HT) reaction, λ_+, is determined as the sum of the reorganization energies of the donor and acceptor. By definition, λ_1 associated with the removal energy of a hole from the donor state and λ_2 associated with the addition energy of a hole to the acceptor state, λ_+ can be written as [12]

$$\lambda_+ = \lambda_1 + \lambda_2 = \left(E_+^* - E_+\right) + \left(E^* - E\right), \tag{5}$$

where E is the energy of the neutral state in the neutral geometry, E^* is the energy of the neutral state in the radical cation geometry, E_+ is the energy of the radical cation state in the radical cation geometry, and E_+^* is the energy of the radical cation state in the neutral geometry.

2.2 Electronic coupling

The electronic coupling term is defined as the Hamiltonian matrix element between two diabatic states:

$$V_{12} = \langle \eta_1 | H | \eta_2 \rangle. \tag{6}$$

In hole transport cases, η_1 and η_2 are the diabatic states for the cation and neutral dimer, which correspond to the states before and after electron transfer occurs, respectively. Since the direct quantum chemical evaluation for diabatic states is rather difficult, the coupling is usually obtained using the one-electron approximation. Using ab initio or semiempirical quantum chemical methods, various computational techniques for calculating the coupling have been developed [13, 14]. In this work, we used two different methods.

The first is the energy splitting in dimer (ESD) method. In this method, the intermolecular electronic coupling V is evaluated within the framework of a Marcus–Hush

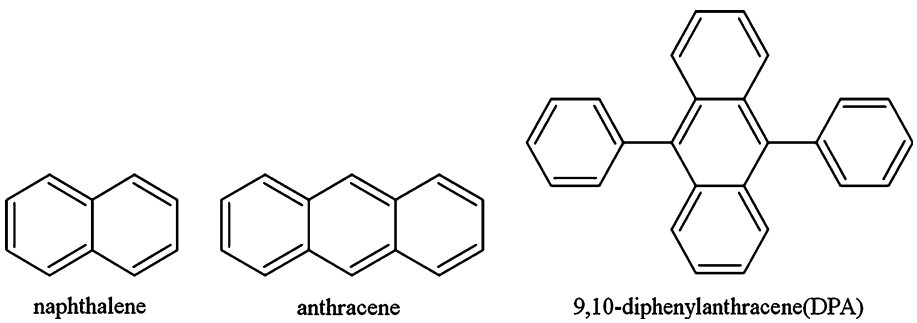

Fig. 1 Chemical structures of naphthalene, anthracene, and 9,10-diphenylanthracene

two-state model [3, 9, 10]. For a neutral dimer system, the HOMO of the isolated molecule splits into two levels, denoted as HOMO and HOMO-1. Then, the electronic coupling is given by

$$V_{+}^{\mathrm{ESD}} = \frac{1}{2}(E_{\mathrm{HOMO}} - E_{\mathrm{HOMO-1}}), \tag{7}$$

where E_{HOMO} and $E_{\mathrm{HOMO\text{-}1}}$ are the dimer orbital energies of HOMO and HOMO-1, respectively.

The second method of evaluating electronic coupling is the site-energy corrected splitting scheme proposed by Valeev et al. [15]. Hereafter, we call the second method the charge transfer integral (CTI) method. To calculate the charge transfer integral in hole-transfer cases, the monomer HOMOs localized at sites 1 and 2, i.e., $\varphi_{\mathrm{HOMO}}^{\mathrm{C1}}$ and $\varphi_{\mathrm{HOMO}}^{\mathrm{C2}}$, respectively, are used as the basis set for the Hamiltonian of the dimer system. On a symmetrically orthonormalized basis [16, 17], intermolecular electronic coupling is evaluated from the charge transfer integral (J_{DA}), the spatial overlap (S_{DA}) between the donor and acceptor sites, and the site energies (H_{DD}, H_{AA}):

$$V_{+}^{\mathrm{CTI}} = \frac{J_{\mathrm{DA}} - S_{\mathrm{DA}}(H_{\mathrm{DD}} + H_{\mathrm{AA}})/2}{1 - S_{\mathrm{DA}}^2} \tag{8}$$

$$J_{\mathrm{DA}} = \langle \varphi_{\mathrm{HOMO}}^{\mathrm{C1}} | h_{\mathrm{KS}} | \phi_{\mathrm{HOMO}}^{\mathrm{C2}} \rangle$$

$$S_{\mathrm{DA}} = \langle \varphi_{\mathrm{HOMO}}^{\mathrm{C1}} \mid \varphi_{\mathrm{HOMO}}^{\mathrm{C2}} \rangle$$

$$H_{\mathrm{DD}} = \langle \varphi_{\mathrm{HOMO}}^{\mathrm{C1}} | h_{\mathrm{KS}} | \varphi_{\mathrm{HOMO}}^{\mathrm{C1}} \rangle$$

$$H_{\mathrm{AA}} = \langle \varphi_{\mathrm{HOMO}}^{\mathrm{C2}} | h_{\mathrm{KS}} | \varphi_{\mathrm{HOMO}}^{\mathrm{C2}} \rangle,$$

where h_{KS} is the Kohn–Sham one-electron Hamiltonian of the dimer system. A similar procedure for electronic coupling was proposed by Yang et al. [18], which is called the direct charge transfer integral method. The only difference between Valeev et al. [15] and Yang et al. [18] is in the one-electron Hamiltonian form h_{KS}, the former method uses the real dimer density with h_{KS}, whereas the latter one uses the noninteracting monomer densities as the dimer density.

2.3 Quantum chemical calculations

To determine each charge transfer parameter, we used the density functional calculation with the hybrid B3LYP functional set [19–21]. The calculation of radical cation states was carried out by the unrestricted DFT scheme. Geometry optimization was performed with the Gaussian 03 program [22]. All the other calculations were performed with the DFT program developed in our laboratory [23–26]. In all the present DFT calculations, the 6-31G(d) basis set was used.

Reorganization energy was obtained by calculating four energies using Eq. 5 with optimized structures for the neutral and radical cation states. For the DPA, the neutral and radical cation structures were optimized with the dihedral angle between the anthracene backbone and the phenyl groups fixed at 66.8° in the crystal.

As mentioned above, the electronic couplings of all the dimer pairs were evaluated by the ESD and CTI methods. In the electronic coupling calculation, the geometries used are the experimental ones, and the geometries of the dimer pairs were selected from X-ray crystal structures.

3 Results and discussion

3.1 Reorganization energy

Reorganization energy can be determined from the relaxation process for neighboring donor and acceptor species. The vertical and adiabatic ionization potentials IP_v and IP_a and the hole-extraction potential HEP associated with this process are given by [27]

$$\mathrm{IP}_v = E_{+}^{*} - E$$

$$\mathrm{IP}_a = E_{+} - E$$

$$\mathrm{HEP} = E_{+} - E^{*}.$$

HEP corresponds to the vertical electron affinity of radical cation species. Thus, the reorganization energy of Eq. 5 can be redefined as

$$\lambda_{+} = \mathrm{IP}_v - \mathrm{HEP}. \tag{9}$$

The reorganization energies, ionization potentials, and hole-extraction potentials estimated by DFT calculations are shown in Table 1. The reorganization energy of anthracene is smaller than that of naphthalene, which shows that the structure relaxation in the HT reaction becomes smaller as the conjugate system extends (Fig. 2).

DPA has a reorganization energy of 0.1535 eV, which is larger than that of anthracene but less than that of naphthalene. The small reorganization result for DPA comes from the HOMO distribution. As shown in Fig. 3, the π type HOMO of DPA is mainly localized on the anthracene backbone, whereas the π electron slightly flows to the phenyl ring moieties owing to ring twisting. Namely, with respect to the relaxation energy of anthracene, the extra

Table 1 Reorganization energies of naphthalene, anthracene, and DPA

	Naphthalene	Anthracene	DPA
λ_{+} (eV)	0.1856	0.1381	0.1535
IP_v (eV)	7.6874	6.8730	6.4252
IP_a (eV)	7.5945	6.8036	6.3485
HEP (eV)	7.5018	6.7350	6.2717

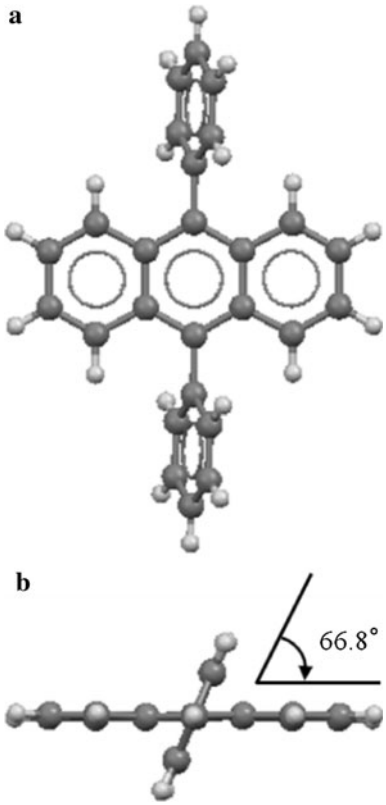

Fig. 2 **a** DPA monomer in single crystal and **b** side view of part (**a**)

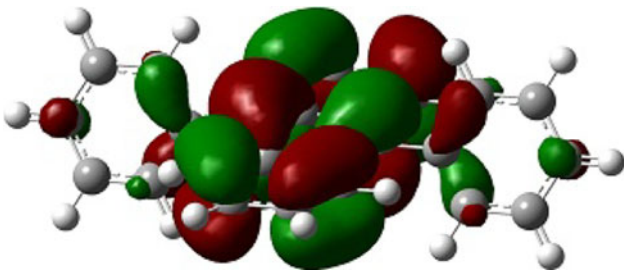

Fig. 3 HOMO of DPA

relaxation energy of DPA is required only for the structural relaxation of two phenyl groups. On the other hand, DPA shows the smallest ionization potential among the three molecules, as shown in Table 1. According to Eq. 9, we can simply estimate that compounds with small ionization potentials also have low reorganization energies. Nevertheless, DPA shows the higher reorganization energy than anthracene, which comes from the fact that DPA has the smallest HEP among the three systems.

3.2 Electronic coupling and mobility

The crystal parameters of naphthalene, anthracene, and DPA are summarized in Table 2. The crystal structure of anthracene is shown in Fig. 4. Four type (eight) dimers,

Table 2 Cell parameters of naphthalene [28], anthracene [29], and DPA [32]

Space group	Naphthalene $P2_1/a$	Anthracene $P2_1/a$	DPA $C2/c$
a (Å)	8.213	8.553	10.683
b (Å)	5.973	6.016	13.552
c (Å)	8.675	11.172	12.257
α (°)	90.00	90.00	90.00
β (°)	123.39	124.60	90.54
γ (°)	90.00	90.00	90.00

namely, T_1, T_2, P, and L, were selected as the hopping route in this crystal. As for the naphthalene, we treated it in a similar manner. For the naphthalene and anthracene systems, the electronic couplings calculated by the ESD and CTI methods, and the hole mobilities predicted using Eqs. 1–4 are shown in Table 3. It can be seen from Table 3 that via the ESD method, the hole mobilities of naphthalene and anthracene are 2.17 and 5.18 $cm^2/(Vs)$, respectively. This shows that the ESD method overestimates the hole mobility by about twofold compared with the experimental values [30, 31]. On the other hand, in the case of the CTI method, the predicted hole mobilities of naphthalene and anthracene are 0.35 and 1.39 $cm^2/(Vs)$, respectively. Thus, the CTI results fall within the range of experimental results, whereas the ESD results do not.

In Table 3, the large difference in electronic coupling between the ESD and CTI methods can be seen in the results of the tilted dimers, V_{T1} and V_{T2}. In such a face-to-edge dimer, the electronic state for the face monomer is strongly polarized by the electrostatic interaction due to the edge monomer, as tilted angle increases. As shown in a previous work [15], the energy splitting between the dimer HOMO and HOMO-1 for Eq. 7 can be written as the square root of the sum of two squared terms. The first term is the energy splitting Δe_{AD} between the donor and acceptor HOMOs under a symmetrically orthonormalized basis set, and the second term is the charge transfer integral V_+^{CTI} of Eq. 8:

$$\Delta E = E_{HOMO} - E_{HOMO-1} = 2V_+^{ESD} = \left\{ (\Delta e_{AD})^2 + (2V_+^{CTI})^2 \right\}^{1/2}. \quad (10)$$

We can see from Eq. 10 that the ESD coupling term corresponds to the CTI coupling term only if the absolute value of Δe_{AD} is negligible. For the T_1 and T_2 dimers in Table 3, Δe_{AD} becomes the dominant term of the dimer orbital energy difference ΔE, and the transfer integral term V_+^{CTI} contributes less to ΔE. Then, the ESD method performed with Eq. 6 tends to overestimate the electronic coupling for the tilted dimers V_{T1} and V_{T2}. The results in Table 3 well confirm the previous caution for the practical

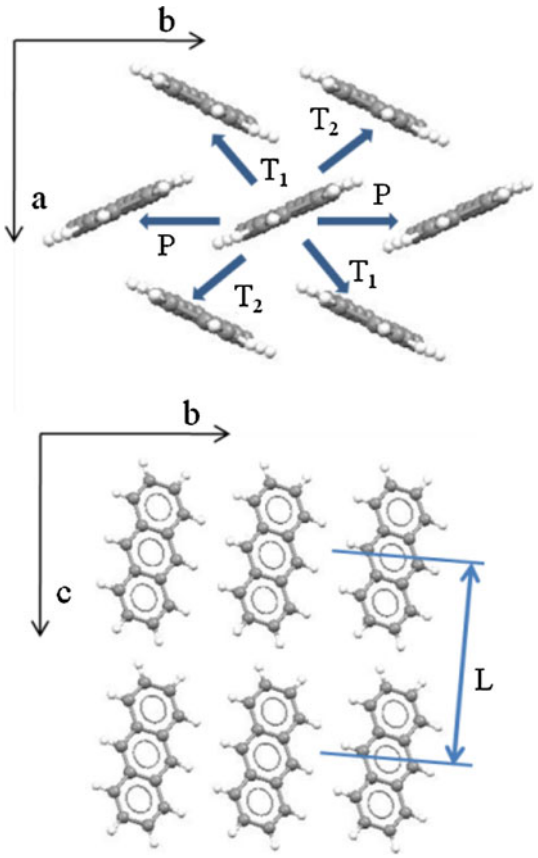

Fig. 4 Crystal structure of anthracene, **a** *ab*-plane and **b** *bc*-plane

Table 3 Electronic couplings and hole mobilities of naphthalene and anthracene

		Naphthalene		Anthracene	
		ESD	CTI	ESD	CTI
r_{T1} (Å)		5.077		5.228	
V_{T1} (eV)		0.144	0.00983	0.16	0.0321
r_{T2} (Å)		5.077		5.228	
V_{T2} (eV)		0.144	0.00983	0.16	0.0321
r_p (Å)		5.973		6.016	
V_p (eV)		0.0331	0.0504	0.0424	0.0799
r_L (Å)		8.675		11.17	
V_L (eV)		0.00068	0.000917	0.0	0.000186
μ_+ [cm^2/(Vs)]	This work	2.17	0.35	5.18	1.39
	Exptl.	0.4–1[a]		0.57–2.07[b]	

[a] Cited from Karl [30]

[b] Cited from Silinsh and Capek [31]

application of the ESD method to real organic semiconductor systems [15]. In this study, we did not consider the embedding effects on the electronic coupling in the single-crystal systems. Valeev et al. [15] concluded that the electronic coupling obtained from the CTI method for isolated dimers and for dimers embedded in a crystal environment practically coincide owing to a near-complete cancellation of equivalent dimer interactions. The embedding effects may not be critical in the present results.

From the electronic couplings by the CTI method, in naphthalene and anthracene, the P dimer has the largest contribution to their mobilities. The electronic couplings of the T_1 and T_2 dimers are considerably small in naphthalene. On the other hand, in anthracene, those of the T_1 and T_2 dimers are about half of that of the P dimer. Because of the small contribution of the L dimer to the mobility, the hole transfer is expected to occur almost in the (*ab*)-plane.

Using the crystal parameters [32] in Table 2, the electronic couplings and the hole mobility for DPA are summarized in Table 4. The four neighboring-type (eight) dimers are selected as the hopping route in the DPA crystal; two parallel dimer types, i.e., the P_1 and P_2 dimers, where the anthracene backbones are mutually parallel, and two tilted dimer, i.e., the T_1 and T_2 dimers (Fig. 5). The hole mobility determined by the ESD method is 0.37 cm^2/(Vs), which is one-tenth of the experimental value [7]. Since the ESD results underestimate the hole mobility, the site-energy contribution to the difference between the dimer HOMO and HOMO-1 is not important. In the CTI method, the predicted value is 2.15 cm^2/(Vs), which is close to the experimental value of 3.7 cm^2/(Vs) in comparison with the ESD result. These results show that the crystal structure of DPA is more complex than that of naphthalene and anthracene, and that the orbitals of the DPA dimer HOMO and HOMO-1 cannot suitably be described by the simple HOMO–HOMO interaction between DPA monomers.

As seen from the electronic coupling calculated by the CTI method (Table 4), the P_2 dimer shows the largest contribution in mobility ($V_+^{CTI} = 0.07474$ eV). The structure of

Table 4 Electronic couplings and hole mobilities of DPA

		DPA	
		ESD	CTI
r_{T1} (Å)		8.092	
V_{T1} (eV)		0.00981	0.01073
r_{T2} (Å)		8.168	
V_{T2} (eV)		0.02653	0.06095
r_{P1} (Å)		8.628	
V_{P1} (eV)		0.0	0.00038
r_{P2} (Å)		8.628	
V_{P2} (eV)		0.03116	0.07474
μ_+ [cm^2/(Vs)]	This work	0.37	2.15
	Exptl. [7]	3.7	

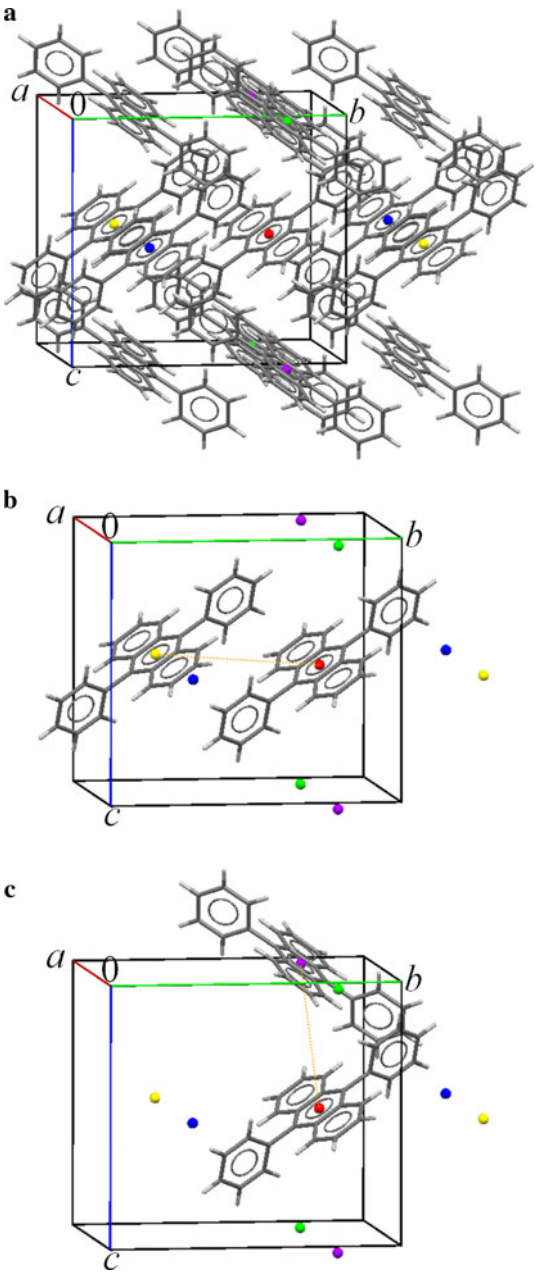

Fig. 5 **a** Crystal structure of DPA, **b** P_2 dimer, and **c** T_2 dimer, where nine *color* spheres in each figure indicate the mass centers of DPA *red* (unit cell center), *blue* (P1), *yellow* (P2), *green* (T1), and *violet* (T2)

the P_2 dimer indicates a small distance between the anthracene backbone of site 1 and phenyl group of site 2 (the smallest C–C contact distance of 3.673 Å). Since the phenyl ring at site 1 is very close to the anthracene backbone, the phenyl rings can polarize the π system of anthracene at other sites. Thus, the typical face-to-edge interaction between neighboring sites can be expected for the P_2 dimer, adding to the face-to-face interaction between anthracene backbones. The T_2 dimer showed the next largest coupling ($V_+^{\mathrm{CTI}} = 0.06095$ eV), whose magnitude is comparable to that of the P_2 dimer. The T_2 dimer structure indicates a small distance between phenyl groups of sites 1 and 2 (the smallest C–C contact distance of 3.785 Å). It is thought that phenyl groups are responsible for the high hole mobility in a DPA single crystal. For the P_1 and T_1 dimers, their contributions to mobility are small.

The CTI results show that the high mobility of DPA comes from the high electronic coupling of the P_2 dimer, where the HOMO of site 1 slightly penetrates the twisting phenyl group (see Fig. 3) and can overlap with the major part of HOMO on the anthracene backbone of site 2. Thus, it is shown that, in the DPA crystal, the twisting motion of two phenyl groups plays an important role in including a high mobility.

We showed that CTI electronic coupling gives better results for hole mobilities than ESD coupling. From a quantitative viewpoint of DPA hole mobility, however, there is a large gap between the theoretical and experimental values, namely, 2.15 and 3.7 $cm^2/(Vs)$, respectively. Thus, what points should we improve for the quantitative prediction of hole mobility? Firstly, in the calculations of the reorganization energies λ_i and electronic coupling V_i, we used a relatively small basis set, 6-31G(d). Employing a larger basis set will improve the theoretical values. Secondly, in this study, the commonly used B3LYP hybrid exchange-correlation functional was used to calculate λ_i and V_i. Probably, using new and more accurate exchange-correlation functionals [33] can lead to an improvement in the quantitative accuracy on the mobility predictions. Thirdly, to obtain the exact charge hopping rates W_i in Eq. 2, we need to calculate the Marcus parameters λ_i and V_i more quantitatively. Thus, we may need to abandon the one-electron approximation for electronic coupling. Using constrained DFT (CDFT) [34], we have attempted to calculate the properties for several electron transfer systems [35]. By using CDFT calculations the diabatic states for a charge transfer complex are directly obtained and more reliable electronic couplings using Eq. 6 are obtained without using the one-electron approximation. The application of CDFT calculations for the determination of hole mobilities for single-crystal systems is under way. Finally, quantitative analysis of the theoretical and experimental values is possible by the investigation of anisotropic hole mobility as has been shown by Wen et al. [36].

4 Conclusions

The hole mobility of DPA was investigated by DFT calculations. Compared with the single-crystal structures of naphthalene and anthracene, that of DPA reveals a higher transport property. In predicting hole mobility, reorganization energy and electronic coupling are important. In

particular, for electronic coupling evaluation, both ESD and CTI methods were examined. The CTI method qualitatively reproduces experimental results, whereas ESD overestimates electronic coupling for naphthalene and anthracene and underestimates electronic coupling for DPA. The results obtained support those of a previous study [15].

The electronic coupling calculation via the CTI method shows that the high-charge transfer property of DPA comes from the face-to-edge interaction between the anthracene backbone of one DPA site and the twisted phenyl groups of a neighboring DPA site. Evidently, such a significant face-to-edge interaction between neighboring sites can be a common characteristic in organic semiconductor systems such as rubrene with excellent charge transfer property.

References

1. Brédas JL, Beljonne D, Coropceanu V, Cornil J (2004) Chem Rev 104:4971–5003
2. Coropceanu V, Cornil J, da Silva Filho DA, Olivier Y, Sibey R, Brédas JL (2007) Chem Rev 107:926–952
3. Deng WQ, Goddard WA (2004) J Phys Chem B 108:8614–8621
4. Wen SH, Li A, Song J, Deng WQ, Han KL, Goddard WA (2009) J Phys Chem B 113:8813–8819
5. Irfan A, Zhang J, Chang Y (2010) Theor Chem Acc 127:587–594
6. Gang H (2010) Theor Chem Acc 127:759–763
7. Tripathi AK, Heinrich M, Siegrist T, Pflaum J (2007) Adv Mater 19:2097–2101
8. Sundar VC, Zaumseil J, Podzorov V, Menard E, Willett RL, Someya T, Gershenson ME, Rogers JA (2004) Science 303:1644–1646
9. Marcus RA (1956) J Chem Phys 24:966–978
10. Hush NS (1958) J Chem Phys 28:962–972
11. Blancafort L, Duran M, Poater J, Salvador P, Simon S, Solà M, Voityuk AA (2009) Theor Chem Acc 123:29–40
12. Berlin YA, Hutchison GR, Rempala P, Ratner MA, Michl J (2003) J Phys Chem A 107:3970–3980
13. Newton MD (1991) Chem Rev 91:767–792
14. Li H, Brédas JL, Lennartz C (2007) J Chem Phys 126:164704
15. Valeev EF, Coropceanu V, da Silva Filho DA, Salman S, Brédas JL (2006) J Am Chem 128:9882–9886
16. Löwdin PO (1950) J Chem Phys 18:365–375
17. Senthilkumar K, Grozema FC, Guerra CF, Siebbeles LDA (2003) J Chem Phys 119:9809–9817
18. Yang X, Li Q, Shuai Z (2007) Nanotechnology 18:424029
19. Becke AD (1988) Phys Rev A 38:3098–3100
20. Lee C, Yang W, Parr RG (1988) Phys Rev B 37:785–789
21. Becke AD (1993) J Chem Phys 98:5648–5652
22. Frisch MJ, Trucks GW, Schlegel HB, Scuseria GE, Robb MA, Cheeseman JR, Montgomery JA Jr, Vreven T, Kudin KN, Burant JC, Millam JM, Iyengar SS, Tomasi J, Barone V, Mennucci B, Cossi M, Scalmani G, Rega N, Petersson GA, Nakatsuji H, Hada M, Ehara M, Toyota K, Fukuda R, Hasegawa J, Ishida M, Nakajima T, Honda Y, Kitao O, Nakai H, Klene M, Li X, Knox JE, Hratchian HP, Cross JB, Adamo C, Jaramillo J, Gomperts R, Stratmann RE, Yazyev O, Austin AJ, Cammi R, Pomelli C, Ochterski JW, Ayala PY, Morokuma K, Voth GA, Salvador P, Dannenberg JJ, Zakrzewski VG, Dapprich S, Daniels AD, Strain MC, Farkas O, Malick DK, Rabuck AD, Raghavachari K, Foresman JB, Ortiz JV, Cui Q, Baboul AG, Clifford S, Cioslowski J, Stefanov BB, Liu G, Liashenko A, Piskorz P, Komaromi I, Martin RL, Fox DJ, Keith T, Al-Laham MA, Peng CY, Nanayakkara A, Challacombe M, Gill PMW, Johnson B, Chen W, Wong MW, Gonzalez C, Pople JA (2003) Gaussian 03, revision C.02. Gaussian, Pittsburgh, PA
23. Morihashi K, Shimodo Y, Kikuchi O (2002) J Mol Struct (Theochem) 617:47–52
24. Morihashi K, Shimodo Y, Kikuchi O (2004) Chem Phys Lett 397:461–468
25. Morihashi K, Shimodo Y, Kikuchi O (2005) J Mol Struct (Theochem) 722:169–183
26. Shimodo Y, Morihashi K, Nakano T (2006) J Mol Struct (Theochem) 770:163–168
27. Liu YH, Xie Y, Lu ZY (2010) Chem Phys 367:160–166
28. Brock CP, Dunitz JD (1982) Acta Crystallogr Sect B Struct Sci 38:2218–2228
29. Brock CP, Dunitz JD (1990) Acta Crystallogr Sect B Struct Sci 46:795–806
30. Karl N (2003) Synth Met 133–134:649–657
31. Silinsh EA, Capek V (1994) Organic molecular crystals: interaction, localization and transport phenomena. American Institute of Physics, New York, pp 332–333
32. Becker HD (1992) Z Kristallogr 199:313–315
33. Song J-W, Tsuneda T, Sato T, Hirao K (2011) Theor Chem Acc. doi: 10.1007/s00214-011-0997-6
34. Wu Q, Van Voorhis T (2006) J Chem Phys 125:164105
35. Ogawa T, Sumita M, Shimodo Y, Morihashi K (2011) Chem Phys Lett 511:219–223
36. Wen SH, Li A, Song J, Deng WQ, Han KL, Goddard WA (2009) J Phys Chem B 113:8813–8819